VTT Technical Research Centre of Finland

Oxidative treatment and nanofibrillation softwood kraft fibres with lytic polysaccharide monooxygenases from Trichoderma reesei and Podospora anserina

Marjamaa, Kaisa; Lahtinen, Panu; Arola, Suvi; Maiorova, Natalia; Nygren, Heli; Aro, Nina; Koivula, Anu

Published in:
Industrial Crops and Products

DOI:
10.1016/j.indcrop.2023.116243

Published: 01/03/2023

Document Version
Publisher's final version

Industrial Crops & Products 193 (2023) 116243

Contents lists available at ScienceDirect

Industrial Crops & Products

journal homepage: www.elsevier.com/locate/indcrop

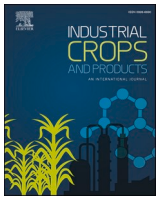

Oxidative treatment and nanofibrillation softwood kraft fibres with lytic polysaccharide monooxygenases from *Trichoderma reesei* and *Podospora anserina*

Kaisa Marjamaa *, Panu Lahtinen, Suvi Arola, Natalia Maiorova, Heli Nygren, Nina Aro, Anu Koivula

VTT Technical Research Centre of Finland Ltd, P.O.Box 1000 02044 VTT Espoo, Finland

ARTICLE INFO

Keywords:
Softwood kraft
Lytic polysaccharide monooxygenase
Oxidation
CNF
Film
Barrier

ABSTRACT

Cellulose oxidation and enzymatic treatments can be employed to reduce the energy consumption in production of cellulose nanofibrils (CNFs). Lytic polysaccharide monooxygenases (LPMOs) offer new biocatalytic tools for oxidative pretreatment of cellulosic fibres in this process. In this work the capability of LPMO enzymes to enhance fibrillation of bleached softwood kraft fibres was studied using two LPMO enzymes, i.e. C1/C4-oxidising AA9A from *Trichoderma reesei* (*Tr* AA9A) and C1-oxidising AA9E from *Podospora anserina* (*Pa* AA9E). The enzymatic treatments were carried out after mechanical pre-refining (grinding) of the pulp, which resulted in clear reduction of the intrinsic viscosity of the refined fibres compared to the previously published work, presumably due to better access of the enzymes on the fibre polysaccharides. The *Tr* AA9A treatments were carried out using different enzyme dosages (0.25–10 mg/g dry fibre) and fixed reaction time (24 h), resulting in fibres characterized by increased aldehyde content, which is in line with the C1/C4 oxidising activity of this enzyme. Comparison of the *Tr* AA9A to *Pa* AA9E with fixed enzyme dosage (2 mg/g dry fibre) and reaction time (24 h), showed that no remarkable increase in total charge of the cellulosic fibres could be obtained with either of the LPMO enzymes in these conditions. All the LPMO pretreatments improved fibrillation of mechanically refined fibres in microfluidization, seen as clearly lower residual fibre content and higher proportion nanosized material. In comparison of the *Pa* AA9E to *Tr* AA9A, clearly faster fibrillation was achieved with the *Pa* AA9E pretreatment. The mechanical and oxygen barrier properties of CNF films prepared from LPMO pretreated fibres were very similar to the reference CNF films while water vapour transmission rate was somewhat higher.

1. Introduction

Cellulose nanofibrils (CNFs) are renewable and biodegradable nanomaterials suitable for diverse applications e.g. in fields of pharmaceuticals, cosmetics, biomedicine, packaging and composites (reviewed e.g. in de Amorim et al., 2020). CNFs can be manufactured from abundant industrial plant fibres, such as softwood and hardwood kraft pulps, by aqueous mechanical disruption which delaminates the cell walls and releases the cellulose fibrils and fibril bundles with typical diameter of 5–50 nm and length of 50 nm–3 μm (reviewed in Nechyporchuk et al., 2016). The mechanical disintegration of plant fibres requires substantial amount of energy and consequently there has been intense research and development on pretreatment technologies for enhancing the fibrillation. The separation of fibrils can be facilitated by carboxylation, sulfonation, carboxymethylation or quaternization, which introduce electrostatic repulsion between the fibrils (Saito et al., 2006; Aulin et al., 2010, 2009; Liimatainen et al., 2013, 2012). In particular, oxidative carboxylation by a stable nitroxyl radical, (2,2,6,6-tetramethylpiperidin-1-yl)oxyl (TEMPO) has been extensively studied and also commercialized (Isogai, 2018; Isogai et al., 2011).

In nature, the disintegration of cellulosic fibres is facilitated by various microbial enzymes, which catalyse hydrolysis or oxidation of the polysaccharides (reviewed by Østby et al., 2020). Enzymatic catalysis has established applications in lignocellulose saccharification in biofuel sector, as well as in bleaching and refining of cellulosic fibres (reviewed in Marjamaa and Kruus, 2018). Pääkko et al. (2007) and Henriksson

* Corresponding author.
E-mail addresses: kaisa.marjamaa@vtt.fi (K. Marjamaa), panu.lahtinen@vtt.fi (P. Lahtinen), suvi.arola@vtt.fi (S. Arola), natalia.maiorova@vtt.fi (N. Maiorova), heli.nygren@vtt.fi (H. Nygren), nina.aro@vtt.fi (N. Aro), anu.koivula@vtt.fi (A. Koivula).

https://doi.org/10.1016/j.indcrop.2023.116243
Received 21 October 2022; Received in revised form 22 December 2022; Accepted 2 January 2023
Available online 7 January 2023

et al. (2007) have showed that restricted enzymatic hydrolysis, using endoglucanase type of enzyme (EC 3.2.1.4), facilitates mechanical fibrillation of pulps. The endoglucanases hydrolyse internal linkages in cellulose polymer in non-ordered (amorphous) areas in cellulose fibres, which is weakens the integrity of fibres and makes them susceptible to mechanical disassembly. Since the initial finding, there have been several studies on using hydrolytic enzymes in nanocellulose production (reviewed in Pirich et al., 2020) using for instance cellulases (Wang et al., 2015; Kim et al., 2021) or xylanases (Nie et al., 2018a and Nie et al., 2018b).

Lytic polysaccharide monooxygenases (LPMOs, EC 1.14.99.53–56), are a divergent group of monocopper enzymes, which depending on enzyme variant can catalyse oxidative cleavage of different polysaccharides, including cellulose, starch, chitin, glucomannan, xyloglucan and/or xylan (Hemsworth et al., 2015; Hüttner et al., 2019; Lo Leggio et al., 2015; Vaaje-Kolstad et al., 2010). They are classified into auxiliary activity (AA) protein families in Carbohydrate Active enZyme (CAZy) database (http://www.cazy.org/Auxiliary-Activities.html), in which AA9 family represents the fungal cellulose oxidizing LPMOs. The oxidative action of LPMOs was discovered approximately ten years ago in connection with their remarkable ability to improve saccharification of recalcitrant lignocellulosic materials (Harris et al., 2010; Müller et al., 2015). In contrast to endoglucanases, the AA9 family LPMOs can cleave internal linkages in crystalline celluloses, thus facilitating the degradation of most recalcitrant celluloses. Similar to fungal cellulases, some LPMO enzymes have a bimodular structure having a catalytic module linked to a carbohydrate-binding module (CBM), which enhances the binding of the enzyme on insoluble substrate (Hansson et al., 2017; Chalak et al., 2019). Prerequisites for the LPMO activity are reduction of the active site copper, e.g. by low molecular weight phenolic compounds, pigments or dehydrogenase enzymes (Cannella et al., 2016; Langston et al., 2011; Quinlan et al., 2011), and availability of either molecular oxygen (Vaaje-Kolstad et al., 2010; Frandsen et al., 2016; Meier et al., 2018) or, as more recently discovered, hydrogen peroxide (Bissaro et al., 2017) as co-substrate. The typical LPMOs reaction involves hydroxylation of the glucose units at C1 and/or C4 carbon, leading to cleavage of the $\beta-1,4$-glycosidic linkages and resulting to a terminal aldonolactone (C1-oxidation) at the reducing end and/or ketone (C4-oxidation) at the non-reducing end, respectively. In water, the aldonolactone is spontaneously hydrolysed to aldonic acid, and ketone undergoes reversible transformation to gemdiol, forming an equilibrium.

The capability of LPMOs to oxidize polysaccharides is an intriquing property in modification of cellulosic fibres for material applications (Villares et al., 2017; Hu et al., 2018; Koskela et al., 2019). The *Tr* AA9A LPMO from the filamentous fungus *Trichoderma reesei* (Karlsson et al., 2001; Saloheimo et al., 1997) is known to oxidize the glucose units of cellulose both at C1 and C4 positions, with a preference to the C4 position (Hansson et al., 2017; Pierce et al., 2017; Song et al., 2018; Tanghe et al., 2015; Marjamaa et al., 2022), when suitable electron donor and molecular oxygen and/or hydrogen peroxide are supplied (Kont et al., 2020, 2019). We have recently discovered that oxidative pretreatment of softwood kraft fibres with the *Tr* AA9A enhances solubility of the fibres in cellulose solvent, a phenomenon which can have significance in production of regenerated textile fibres and cellulose derivatives (Ceccherini et al., 2021; Marjamaa et al., 2022).

In the present work, we have studied the capability of two bimodular LPMO enzymes, the C1/C4 oxidising LPMO *Tr* AA9A and the C1-oxidising *Pa* AA9E from *P. anserina* (Bennati-Granier et al., 2015), to enhance fibrillation of bleached softwood kraft fibres in microfluidization. Different enzymes dosages of *Tr* AA9A, comparison of *Tr* AA9A to *Pa* AA9E as well as the combined effect of the *Tr* AA9A and *Pa* AA9E were evaluated. The enzymatic treatments were applied on mechanically pre-refined fibres and the effect of enzymatic treatment on the fibres was followed by spectrophotometric aldehyde quantification, intrinsic viscosity measurements and conductometric titration. The soluble sugars were analysed with a liquid chromatography method that we have developed for analysing oligosaccharide mixtures arising from the oxidative enzyme treatments. The quality of fibrillated pulps was assessed via rheology, optical methods as well as light and scanning electron microscopy (SEM), and finally free-standing films were casted from the mechano-enzymatically fibrillated cellulose samples and characterized for their barrier properties. Samples prepared without enzymatic pretreatment were used as a reference in all the experiments.

2. Materials and methods

2.1. Cloning, expression, production and purification of the enzymes

Tr AA9A LPMO enzyme was produced in *T. reesei* and purified as described previously (Kont et al., 2019). *P. anserina* AA9E expression plasmid, pFiDi05 was constructed as follows: The synthetic gene (cDNA) encoding *Pa* AA9E (Uniprot accession number B2ATL7) was codon optimized for *T. reesei* and synthesized at GeneArt (Thermo). The synthetic gene was cloned by yeast recombination into expression vector, pTTv248, containing *cbh1* promoter, terminator, hygromycin selection marker, and targeting sequence for the *cbh1* locus (Colot et al., 2006). After plasmid rescue from yeast the plasmid was transformed into Top10 *E. coli* cells and selected on ampicillin plates. The correct assembly was verified by restriction enzyme analysis. The expression cassette was released from the pFiDi05 plasmid with *Pme*I restriction enzyme and purified from agarose gel. The cassette was transformed to protease deficient and cellulase negative *T. reesei* strain M2184 essentially as described Penttilä et al. (1987) and transformants were selected for hygromycin resistance on plates containing 125 μg/mL of hygromycin B. M2184 is a cellulase deletion strain generated from M124 strain by sequentially deleting 10 secreted proteases; *pep1* (tre74156), *tsp1* (tre73897), *pep4* (tre77579), *gap1* (tre69555), *slp1* (tre51365), *pep3* (tre121133), *pep5* (tre81004), *pep2* (tre53961), *amp2* (tre108592) and *slp8* (tre58698) and six secreted hydrolases *cel6a* (72567), *cel7b* (122081), *cel5a (120312)*, *xyn2* (123818), *cel45a* (49976) and *cel61a* (73643) (as described before in Fang et al., 2017; Landowski et al., 2015). The gene identifiers are listed according to the Joint Genome Institute *T. reesei* assembly release version 2.0 (https://mycocosm.jgi.doe.gov/Trire2/Trire2.home.html). The fragments used for deletion contained the 5′ and 3′ flanking regions of the target gene, a *pyr4* selection marker with a loop-out fragment. Transformants of pFiDi05 were screened by PCR for correct integration of the constructs to the *cbh1* locus and deletion of *cbh1* ORF.

Five *T. reesei* transformants with correctly integrated expression cassette were grown in 24 well plates for five days at 28 °C in *T. reesei* mineral medium (TrMM) plus 40 g/L lactose, 20 g/L spent grain extract, 8.6 g/L diammonium citrate, 5.4 g/L $NaSO_4$, 100 mM PIPPS at pH 4.5, shaking at 28 °C at 800 rpm (Infors AG). TrMM contains 15.0 g/L KH_2PO_4, 2.4 mM $MgSO_4{\cdot}7\ H_2O$, 4.1 mM $CaCI_2{\cdot}H_2O$, 3.7 mg/L $CoCI_2$, 5 mg/L $FeSO_4{\cdot}7\ H_2O$, 1.4 mg/L $ZnSO_4{\cdot}7\ H_2O$, and 1.6 mg/L $MnSO_4{\cdot}7\ H_2O$ and 1 mM $CuSO_4{\cdot}7\ H_2O$. All the five *T. reesei* transformants secreted the *Pa* AA9E protein into the culture medium. The highest producing transformant was purified through single colony plating and named M2495. Spore suspensions were prepared by cultivating the fungus on potato-dextrose plates (BD, Sparks, Maryland, USA) for 5 days, after which the spores were harvested, suspended in a buffer containing 0.8% NaCl, 0.025% Tween-20% and 20% glycerol, filtered through cotton, and stored at − 80 °C.

For *Pa* AA9E production, the *T. reesei* strain M2495 was cultivated in Biostat B2 bioreactor, using 1.5 L starting volume (cultivation code FEF-4). The culture medium was composed of lactose (60 g/L), distiller's spent grain (30 g/L), KH_2PO_4 (5 g/L), $(NH_4)_2SO_4$ (5 g/L), $MgSO_4 \times 7\ H_2O$ (0.59 g/L), trace elements (Fang et al., 2017), 1 mL/L) and antifoam Struktol J673 (2 mL/L), 2 mM $CuSO_4$ and 4 mM $CaCl_2$ and pH of the medium was adjusted to 4.8. The cultivation was carried out at 28 °C for 85.9 h. Lactose (20%) was fed to the culture after batch sugars were

consumed (after 3 d of culture). After cultivation the solids were removed by centrifugation and the liquid was stored at − 20 °C. Protein concentrations in the culture supernatant were measured with BioRad DC kit and with bovine serum albumin (BSA) standards according to manufacturer's instructions (BioRad, USA). The culture supernatant samples were pre-purified with trichloroacetic acid (TCA) precipitation prior protein analysis. This was done by mixing the samples 1:1 with 10% TCA, followed by incubation at 4 °C for 0.5 h. The precipitates were collected by centrifugation (140,000 rpm, 10 min), and redissolved in Lowry A reagent (2% Na_2CO_3, 4% NaOH).

For protein purification, the culture supernatant FEF4 was filtered through GF/A filter and the changed to 20 mM sodium acetate buffer pH 5 using Sephadex G25 gel filtration column (3 L volume) in two 540 mL aliquots. The 1949 mL sample was applied in equilibrated CM Sepharose column (volume 2.1 L) using flow rate of 200 mL/min, and unbound protein was washed with eight columns volumes (CV) of the 20 mM sodium acetate buffer pH 5. The bound proteins were eluted with 0–0.32 mM sodium chloride gradient (16 column volumes) and collecting 700 mL fractions. The fractions were analysed with Criterion Stain Free SDS-PAGE gels (BioRad, USA) and the ones enriched with *Pa* AA9E protein were combined in two pools, and desalted and concentrated with Pellicon ultrafiltration system with 5 kDa cut-off membrane from 9300 mL to 525 mL and 6200–490 mL. pH of the samples was adjusted to 6.2 with 0.5 M Na_2HPO_4 and the samples were applied into 100 mL CM Sepharose column equilibrated with 10 mM sodium phosphate buffer pH 6.2. The *Pa* AA9E was collected from the flow through, while impurities were retained. Ammonium sulphate was added to the samples in 1 M concentration and the samples were applied into 50 mM Phenyl Sepharose column equilibrated with 20 mM sodium acetate buffer pH 5 containing 1 M ammonium sulphate. The bound protein was eluted with 10 mM sodium acetate buffer pH 5, pooled and changed to 20 mM sodium acetate buffer pH 5 using 400 mL Sephadex G25 column. The concentrations of purified enzyme was analysed by measuring absorbance at A280 nm. The purified enzyme was stored in − 20 °C.

2.2. Pulps

Two different pulp types were used for enzymatic treatment and fibrillation trials. The once-dried bleached softwood kraft (Norway spruce, Scots pine) pulp was received as dry sheets from Metsä Fibre Rauma mill. The sheets were wetted and disintegrated to separate fibres according to SCAN-C 18:65 (except that the pulp concentration was 50 g (dry matter) /2.5 L of water) and the wetted pulp was washed to sodium form prior use as described in Rahikainen et al. (2019) and Swerin et al. (1990), respectively. The dry matter content of the disintegrated and washed pulp was 24.3%. Never-dried bleached softwood pulp was obtained from Metsä Fibre Rauma mill in wet form in 39% dry matter content. The never-dried pulp was also washed to sodium form.

The pulp suspensions were diluted to 2% consistency and pre-refined once in a grinder (Supermasscolloider MKZA10–15 J, Masuko Sangyo Co., Japan) at 1500 rpm. Energy consumption was approximately 2 kWh/kg per dry pulp. Altogether three batches were pre-refined, i.e. one from the once-dried pulp obtained from the mill as dry sheets, and two batches from the never-dried pulps. First trials with varying enzyme dosage (0.25 mg and 2 mg *Tr* AA9A/g dry fibre) were done with the once dried re-wetted and disintegrated bleached kraft pulp. The comparison of 2–10 mg LPMO dosage for *Tr* AA9A and comparison of *Tr* AA9A and *Pa* AA9A were done with the never-dried bleached pulp batches (batch 1 and batch 2, respectively). After pre-refining the pulps were stored in a refrigerator before further modification. Dry matter content in pulps was analysed by oven drying (105 °C, overnight).

2.3. LPMO pretreatments

The mechanically refined softwood kraft fibres were treated with *Tr* AA9A, *Pa* AA9E or their combination. The pulp amount in each treatment was 25 g (dry matter). The protein load in the enzyme treatments was 0.25–10 mg/g dry fibre, in case of treatment with combination of *Tr* AA9A and *Pa* AA9E both enzyme were added 1 mg/g dry fibre. The reaction mixtures contained 1.5% pulp (dry matter) in 50 mM sodium phosphate buffer pH 7 and 1 mM gallic acid (GA) as reductant. The reactions were carried out in 45 °C water bath and with blade mixer. After 24 h incubation, the mixtures were heated 100 ℃ for 20 min to inactivate the enzyme. Liquid and solids were separated by filtration through 60 μm mesh. The first flow through was recirculated through the solids, after the solids were washed with 10 × 20 mL of reverse osmosis water. The liquid samples were stored at − 20 °C until analysis. The solids were stored at 4 °C until analysis and microfluidization. Control reactions were done in each series without the enzyme or without enzyme and GA.

2.4. Fibrillation

Fibrillation followed the method described in Vartiainen et al. (2016) with some exceptions. The pre-refined fibre suspension was processed with a microfluidizer model M110-EH. First cycle was through the chambers having a diameter of 400 μm and 200 μm. Then four cycles were through the 400 μm and 100 μm chambers. Operating pressure was 1100 bar in the first cycle and 1800 bar during four cycles. Hydrogel was produced after five cycles through the microfluidizer and sample collection was done after the third and the fifth microfluidization cycle for further analysis. The total number of fibrillation passes was four and six when pre-refining was included.

2.5. Analysis of soluble sugars

The soluble sugars were analysed using an Acquity UHPLC system (Waters, Milford, MA, USA) and Synapt G2-S mass spectrometer (Waters, Milford, MA, USA) as described in Marjamaa et al. (2022). The chromatography was carried out with HYPERCARB column (Thermo Scientific). Mass spectrometry (MS) in ESI-positive ion mode and traveling wave ion mobility (TWIM) was used for further separation and detection of the oligosaccharides. The oligosaccharides and relative quantities of C1 and C4 oxidized oligosaccharides were analysed using calibration curves made from non-oxidized cello- and xylo-oligosaccharides (0.05–100 μg/mL degree of polymerisation (DP) 2–4, in water).

2.6. Analysis of the pulps after enzymatic treatments

Aldehydes in the pulp samples were analysed in duplicate with TTC assay adapted from Obolenskaya et al. (1991) and as described in detail in Ceccherini et al. (2021). Intrinsic viscosity was analysed according to ISO 5351–1 with a PSL Rheotek equipment (Poulten, Selfe & Lee Ltd, UK) in triplicates. Conductometric titration was carried out according to the SCAN-CM 65:02 method.

2.7. Analyses of the fibrillated pulps

2.7.1. Apparent viscosity

Gel strength and low shear viscosities of the fibrillated samples were measured by a Brookfield rheometer model RVDV-III Ultra and vane spindles according to the method described in Kangas et al. (2019). Measuring consistency was 1.5% for all samples. Average values from 10 rpm shear rate level were selected for comparison and measurements were made in duplicate.

2.7.2. Relative amount of nanomaterial

Nanofibril yield was determined gravimetrically by centrifuging at 10000g for 45 min. The method was similar to (Ahola et al., 2008) with small exceptions. The centrifuge was Eppendorf 5804 R and the samples were first diluted to 1.7 g/L consistency and then mixed with a

stator-rotor dispersing instrument (Ultra-Turrax T18) at 9300 rpm for 10 min. After centrifuging the solids content of the supernatant was determined and its proportion in relation to the solids content of the whole sample was calculated, expressing the relative (%) amount of nanosized fibrils in the total amount of fibrillated sample. The measurements were made in duplicate.

2.7.3. Residual micro-sized fiber particles

Fibre analysis was used for determining the amount of larger residual fibre particles that remain in the hydrogel after fibrillation. This method has been previously described by (Kangas et al., 2019) where characterization of residual fibres from CNF samples was carried out with a Kajaani FibreLab analyser. In this analysis the number of residual fibres per mg of sample and TAPPI fines values were recorded from duplicate measurements.

2.7.4. Morphological analysis by imaging

Qualitative analysis of fibre morphology and the homogeneity of the samples was illustrated by optical microscopy and SEM imaging. The fibrillated samples were dyed with Congo Red solution and further diluted the dyed mixture on the microscope slide (Kangas et al., 2019). SEM imaging was done according to the method described by (Lahtinen et al., 2014). Imaging was based on a high-resolution field emission scanning electron microscope (FE-SEM).

2.8. Film casting and characterisation

Self-standing films were produced from the fibrillated samples with a patented film forming concept (Tammelin et al., 2011) using sorbitol as a plasticizer. The D-sorbitol (Sigma-Aldrich) was dissolved in water to 50% concentration and blended with the fibrillated samples to final sorbitol concentration 30% of the fibre weight. The dispersions were processed with SpeedMixer (DAC 110.1 VAC-p, Hauschild) for 2 min at 1500 rpm under vacuum to remove air bubbles. After air removal the dispersions were casted onto a plastic substrate according to method described by Vartiainen et al. (2016). The samples were dried overnight at ambient conditions and then delaminated from the plastic support.

2.8.1. Mechanical characterization of the films

Mechanical properties of the film samples were determined according to modified SCAN P 38:80 (Paper and board - Determination of tensile properties) as in Vartiainen et al. (2016) with minor exceptions. Each test strip was placed between the grips and the grip distance was 20 mm. Test strip had a width of 15 mm and tensile testing speed was 2 mm/min. The tensile tester Lloyd LS5 was equipped with 100 N load cell. The samples were conditioned in a controlled atmosphere (23 °C / 50% relative humidity (RH)) at least for 24 h prior to testing. The average mechanical values were calculated for six repeat measurements.

2.8.2. Oxygen and water vapour transmission

Oxygen transmission rates (OTR) through the films were determined according to standard ASTM D3985 using Oxygen Permeation Analyser Models 8001 (Systech Instruments Ltd, UK). The test area of the sample was 50 cm^2. Tests were carried out at 23 °C and 50% relative humidity (RH) using 100% oxygen as a test gas. Oxygen permeability (OP) was determined by normalizing the OTR to thicknesses of the films.

Water vapour transmission rates (WVTR) of the films were determined gravimetrically using a modified ASTME-96B (wet cup) procedure. Samples with a test area of 30 cm^2 were mounted on a circular aluminium dish (68–3000 Vapometer EZ-Cups), which contained water. Dishes were stored in test conditions of 23 °C and 50% relative humidity (RH) and weighed periodically until a constant rate of weight reduction was attained. Water vapour permeability (WVP) was determined by normalizing the WVTR to thicknesses of the films.

3. Results and discussion

3.1. Production and purification of the Tr AA9A and Pa AA9A LPMO enzymes

Two fungal LPMOs, *Tr* AA9A and *Pa* AA9E were used in the current study. Both enzymes are composed of AA9 family catalytic module interlinked to a CBM1 family cellulose-binding module. The *Tr* AA9A was overproduced in genetically engineered *T. reesei* and purified as described previously in Kont et al. (2019). For production of *Pa* AA9E, a synthetic gene encoding the enzyme was expressed under lactose inducible promoter from *cbh1* gene in *T. reesei*. The strain was cultivated in bioreactor to achieve sufficient amount of protein for the fibrillation studies. After four days of cultivation, the soluble protein concentration in the culture supernatant was ca 9 g/L (Supplementary Fig 1 A), and a clear band corresponding to the recombinant LPMO was observed in the SDS-PAGE analysis (Supplementary Fig 1B). The enzyme was purified from the culture supernatant via three column chromatography steps. The major protein band in the purified enzyme preparation corresponded to the theoretical molar mass of the *Pa* AA9E (30 kDa) and the protein amount recovered was 389 mg (Supplementary Fig 1 C).

3.2. Oxidation of mechanically pre-refined fibres by Tr AA9A

Tr AA9A was studied in oxidative pretreatment of mechanically pre-refined softwood kraft fibres (rSKF), prior nanofibrillation via microfluidization. The pulp used in this experiment was obtained from the mill as dry sheets, and it was re-wetted and disintegrated to separate the fibres prior mechanical pre-refining with the Supermasscolloider MKZA10–15 J. In the refining, the fibre suspension was subjected to compression and shear forces between the grinder stones, which initiated fibrillation and started to loosen fibres. The enzymatic reactions were carried out at 1.5% dry fibre concentration and using 1 mM GA as electron donor (or reductant) for the LPMO catalysis using previously optimized conditions (pH 7, 45 °C) (Marjamaa et al., 2022).

Effect of *Tr* AA9A treatment (enzyme dosages 0.25 and 2 mg/g dry fibre) on aldehyde and viscosity values of rSKF are shown in Fig. 1. We have previously adopted the spectrophotometric TTC assay for aldehydes as a fast and robust method to follow *Tr* AA9A catalysed oxidation of fibres (Ceccherini et al., 2021; Marjamaa et al., 2022). The *Tr* AA9A catalysed oxidative cleavage at C4-position of the glucose units produces two new cellulose chain ends: a keto group in the non-reducing end and a reducing end aldehyde, and as such the amount of aldehydes is expected to correlate with the C4 oxidative cleavages. In addition, intrinsic viscosity measurements were carried out to follow the effect of oxidative cleavages on the pulp molar mass.

In line with our earlier results, the *Tr* AA9A treatment clearly increased the aldehyde concentration in the pre-refined pulp as compared to the reference (Fig. 1 A). The amount of aldehydes formed in the enzymatic treatment with the lower enzyme dosage (0.25 mg/g dry fibre) was ca two times higher compared to the values obtained in our previous work (ca 35 μmol/g fibres), where the same pulp, without the mechanical pre-refining (i.e. without grinding with the Supermasscolloider MKZA10–15 J), was used as substrate (Marjamaa et al., 2022). The *Tr* AA9A treatment also clearly reduced the rSKF viscosity (Fig. 1). The viscosity values typically correlate with molar mass average (Mw) of the fibre polymers. In our previous work, the effect of *Tr* AA9A on the molar mass of the non-refined kraft fibres was minor, even when much higher enzyme dosage was applied (5 mg/g dry fibre) (Marjamaa et al., 2022). Similarly, only minor effect on cellulose molar mass was obtained when softwood kraft fibres were pretreated with another LPMO, *Pa* AA9H (Villares et al., 2017). The mechanical refining applied in the current work prior the LPMO treatment may have increased accessibility of the LPMO to the bulk of the fibres, leading to the observed remarkable decrease in viscosity and higher amount of aldehydes. This would be in line with previous work with hydrolytic

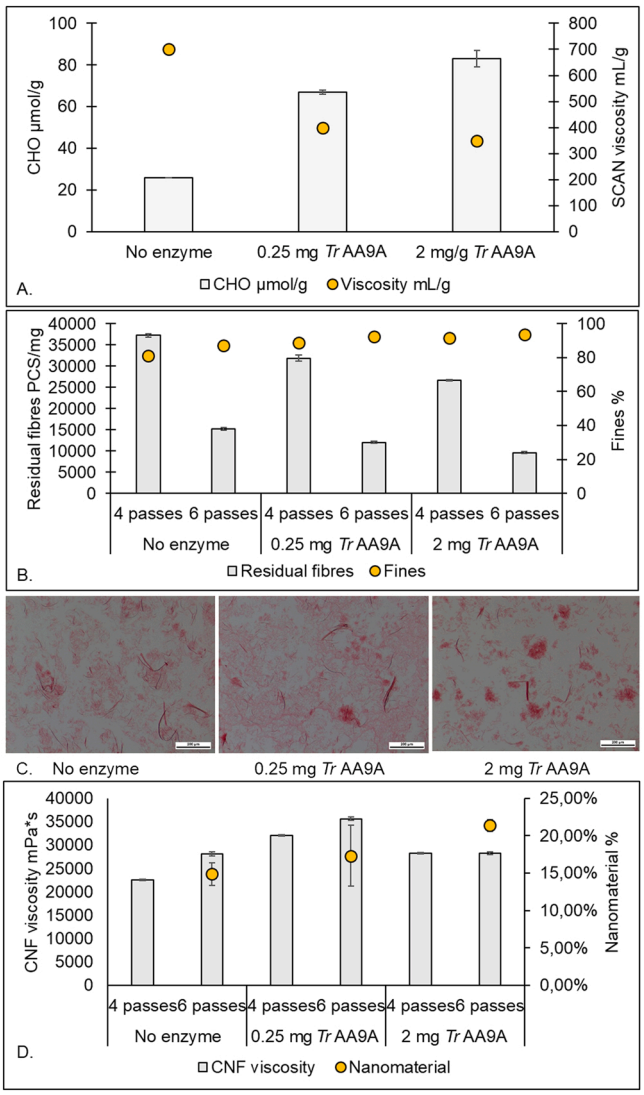

Fig. 1. Oxidation of rSKF by *Tr* AA9A and the effect of the enzymatic treatments on rSKF fibrillation. (A) The oxidation was followed by intrinsic (SCAN) viscosity measurement of the rSKF and quantifying aldehydes in the rSKF with TTC assay. (B) The fibrillation was followed by quantifying residual fibres (PSC/mg) and fines (%) in CNF with FiberLab analyser after 4 and 6 passes of fibrillation. (C) Light microscopy images of Congo Red stained CNFs prepared from the LPMO pretreated fibres and reference fibres (no enzyme in the reaction, only GA). (D) The nanosized material in the CNF (%, dots) was quantified with a centrifugation based-method and the CNF gel viscosity (mPa*s, columns) was analysed with Brookfield rheometer. The enzyme treatments were carried out using 0.25 or 2 mg *Tr* AA9A/g fibre (dry matter), at 1.5% solids loading, in 50 mM sodium phosphate buffer pH 7 and 45 °C for 24 h. The pulp used in the experiment was obtained from the mill as dry sheet, and it was re-wetted, disintegrated to fibres and washed to sodium form prior the mechanical pre-refining and enzymatic pretreatment. No enzyme refers to control reaction containing pulp and GA.

enzymes, where mechanical pretreatment has been shown to enhance cellulase accessibility on wood fibres (Grönqvist et al., 2014; Pääkko et al., 2007).

The LPMO pretreated rSKFs were fibrillated by microfluidization. The fibrillation efficiency was evaluated by analysing the quantity of residual fibres and fines (Fig. 1B), and the products were visually inspected with light microscopy (Fig1C). The *Tr* AA9A treatment enhanced the fibrillation in enzyme dose dependent manner, so that the enzyme pretreated samples contained 37% less residual fibres and 7% more fines than the reference sample (treated with GA only) after six passes of fibrillation (Fig. 1B). Light microscopy images revealed higher amount of visually unstructured aggregates in the LPMO treated fibres, in particular when the higher enzyme dosage was used (Fig. 1C). These are expected to arise from thin fibrils or fines bundled together by the nanosized material (Lahtinen et al., 2014). Relative amount of nanosized material, i.e. % amount of nanofibrils of the total amount of fibrillated material (quantified with the gravimetric method) increased up to 40% compared to the reference. The results suggested that the enzymatic oxidation, seen as increased aldehyde content and reduced intrinsic viscosity of the pulp, enhanced the effect of the mechanical fibrillation (Fig. 1D). Gel viscosity was highest in samples where 0.25 mg *Tr* AA9A was used in the treatment (Fig. 1D). The gel viscosity of the CNFs is affected by fibril morphology (e.g. length, aspect ratio, flexibility) and surface chemistry (reviewed in Hubbe et al., 2017). In case of the sample produced with the 0.25 mg LPMO treatment, the reason for the higher viscosity can be due to the relatively homogenous fibre size distribution and presence of high aspect ratio fibres, which can form strong fibre network under shear. Increasing the enzyme dosage increased the oxidative degradation of the fibres, which may have resulted in shorter fibrils in microfluidization and consequently lower final gel viscosity.

3.3. Oxidation of never-dried refined softwood kraft fibres with higher dosage of Tr AA9A

The effect of further increasing the *Tr* AA9A dosage on oxidation of softwood kraft fibres was studied using never-dried rSKF (batch 1) as substrate in order to maximise the enzyme effect. Drying of the pulp, typically carried out at the mill for storage and transport of the pulp, often has negative effect on efficiency of the enzymatic treatments, due to hornification and consequent reduction of the wettability and accessibility of the substrate (Duan et al., 2015; Imai et al., 2019; Nazhad et al., 1995). The *Tr* AA9A at concentration of 2 mg/g dry fibre produced slightly higher amount of aldehydes to the never-dried rSKF (108 ± 2 µmol/g dry fibre) than rSKF (83 ± 4 µmol/g dry fibre), but increasing enzyme dosage from 2 mg up to 10 mg/g dry fibre had negligible additional effect on the aldehyde concentration and pulp viscosity (Fig. 2 A). The reason for the minor effect of the increasing enzyme concentration could be that the enzyme accessible sites in the fibres were saturated. In addition, the availability of co-substrates, i.e. oxygen or hydrogen peroxide, could have been limiting the oxidation reaction. Hydrogen peroxide was not added to the reaction, but it can be formed *in situ* by oxidation of LPMO reductants (Bissaro et al., 2017). *Tr* AA9A with dosage of 2 mg/ dry fibre enhanced the fibrillation of never-dried rSKF resulting in 54% less residual fibres, 7% higher amount of fines and nearly two time higher amount of nanosized material in the product, compared to the reference samples (treated without enzymes ± GA) (Fig. 2 A & B). It must be noted that the never-dried rSKF batch was fibrillated in general faster than the once dried rSKF, seen as clearly lower amount of residual fibres both in reference samples and enzyme treated sample. Increasing enzyme dosage above 2 mg/g dry fibres had no further improving effect on the fibrillation and accumulation of nanosized material (Fig. 2B & C). The slight decline in the amount of nanosized material may indicate that the main effect of increasing enzyme dosage was degradation of nanofibrils to soluble sugars. Fibrillated material, short residual fibres and fibril aggregates were seen in the light microscopy analysis (Fig. 3A-C) and SEM imaging revealed fibrils with diameter less than 1 µm (Fig. 3D-F).

3.4. Comparison of Tr AA9A and Pa AA9E in oxidation of never-drier refined softwood kraft fibres

The *Tr* AA9A was compared to *Pa* AA9E in oxidation and fibrillation of the never dried rSKF (batch 2). The *Pa* AA9E has been previously shown to enhance fibrillation of bleached birch kraft fibres (Moreau et al., 2019). The soluble oxidation products released in the enzymatic

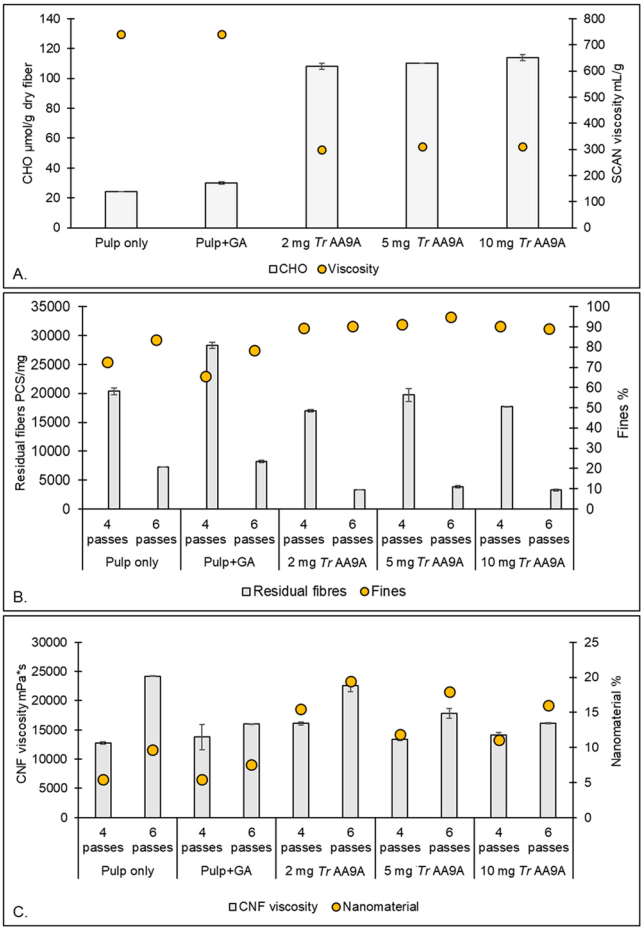

Fig. 2. Oxidation of never-dried rSKF (batch 1) by *Tr* AA9A and the effect of the enzymatic treatments on fibrillation. The oxidation was followed by quantifying aldehydes in pulp with TTC assay and intrinsic (SCAN) viscosity measurement (A) and fibrillation was carried out by microfluidization (total 4 or 6 passes of fibrillation) (B). The fibrillation was followed by quantifying residual fibres (PSC/mg) and fines (%) were analysed with FiberLab analyser. (C) The nanosized material in the fibrillated samples (%, dots) was quantified with a centrifugation based-method and gel (CNF) viscosity (mPa*s, columns) was analysed with Brookfield rheometer. The enzyme treatment was carried out using 2, 5 or 10 mg *Tr* AA9A/g dry fibre, at 1.5% solids loading, pH 7 and 45 °C for 24 h.

treatments were analysed with a LC-IM-MS method previously set-up for this purpose (Marjamaa et al., 2022). This method enabled good resolution and detection of non-oxidized and oxidized oligosaccharides within range of DP2-DP4 in semi-quantitative manner. The amount of soluble sugars detected after the LPMO treatments was low, ca 1% of the dry matter of the pulp. Longer oligosaccharides may contribute the yield loss, but those could not be analysed with the used method. The low soluble sugar concentration correlates well with the results reported earlier with LPMO action on softwood fibres (Villares et al., 2017; Koskela et al., 2019).

The detected oxidized gluco-oligosaccharides, i.e. aldonic acids and ketones/gemdiols, were mostly in line with previously published regioselectivities of the two LPMOs: the *Tr* AA9A catalysed both C4 and C1 hydroxylations, whereas the *Pa* AA9E was strictly C1 specific (Table 1). Sugars having masses corresponding to oxidized xylooligosaccharides were also detected (Table 1). Both C1 and C4 oxidized xylooligosaccharides were detected in *Tr* AA9A and *Pa* AA9E treated samples, suggesting that part of them may arise from some unspecific side-reactions, involving reactive oxygen species arising from oxidation of the reductant. Some LPMOs are capable to oxidize xylan bound on cellulose surface, but such activity has to our knowledge not been described for the LPMOs in current study. However, further studies are needed to verify whether or not the *Tr* AA9A and *Pa* AA9E can in fact oxidize also xylans in the softwood. Oligosaccharides having masses corresponding to double-oxidised cello- and xylooligosaccharides were also detected. This could be indicative of structures such as C4-gemdiol in combination with aldonic acid, but the exact molecular structures of these components could not be determined.

Non-oxidized glucooligosaccharides were also observed, in particular in the samples from *Tr* AA9A treatments. In our previous work, it was seen that the formation of the non-oxidised oligosaccharides is related *Tr* AA9A activity in presence of the reductant, suggesting that these may be degradation product of labile C4 oxidized sugars (Marjamaa et al., 2022). Non-oxidised xylooligosaccharides were also detected, possibly arising from minor xylanase impurity in the purified LPMOs, and/or degradation of C4 oxidized xylooligosaccharides.

Comparison of the aldehyde amounts, intrinsic viscosity values and charge of the LPMO treated fibres are shown in Fig. 4. The *Tr* AA9A treatment produced clearly more aldehydes than the treatment with *Pa* AA9E, which is in line with the lack of C4 oxidising activity of *Pa* AA9E (Bennati-Granier et al., 2015) (Fig. 4A). The aldehyde amount in the reference sample (pulp only) and the *Tr* AA9A treated sample (2 mg/g dry fibre) were similar to the corresponding results from the mechanically pre-refined batch 1 (Fig. 2 A). Viscosity value was lowest in samples treated with *Tr* AA9A (353 mL/g), but the viscosities were quite similar in all the enzyme treated samples (353–422 mL/g) (Fig. 4B). The viscosity values in the reference sample (690 mL/g) and the *Tr* AA9A treated sample were also rather similar to the corresponding data from the never dried rSKF batch 1 (740 mL/g and 300 mL/g, respectively). The charge of the pulp was not remarkably higher after treatment of the C1 oxidising LPMO *Pa* AA9E, although increasing the amount of reducing end aldonic acids could be expected as consequence of the C1 oxidation (Fig. 4 C). Charge values were not either reported in Moreau et al. (2019) in which *Pa* AA9E was used in hardwood fibre treatment in conditions similar to the work reported here. Introduction of negative charge to the fibres, such as in the case of TEMPO-oxidation is known to enhance fibrillation due to electrostatic repulsion between the charged fibrils. Further improvement of the LPMO treatment efficiency may thus be needed to enable significant fibre surface carboxylation and better fibril separation.

One reason for minor effect of LPMO treatment on fiber charge may be caused by solubilisation of the charged sugars. Koskela et al. (2019) observed that when softwood holocellulose was treated with C1 oxidizing *Nc* LPMO9F, a LPMO which has no CBM, the resulting fibres had more charge than with LPMO carrying CBM. The higher charge was related to lower amount of soluble sugars, which would support the theory of loss of charge (of the insoluble fibre fraction) via cellulose solubilisation. Chalak et al. (2019) has proposed that CBM restricts the LPMO movement on the cellulose surface, resulting to several consecutive cleavages in close proximity of the bound enzyme, and consequently to relatively high amount of soluble sugars when compared to a LPMO not having a CBM. Both of the LPMO in the current study contained CBM, which may thus promote the solubilizing action.

The combination of *Tr* AA9A and *Pa* AA9E (1 +1 mg/g pulp) produce lower amount of aldehydes than *Tr* AA9A alone (2 mg/g pulp), and very similar viscosity and charge values as the treatment with single enzymes. No obvious synergy between the two types of LPMO enzymes could thus be detected. The aldehydes in the fibres were expected to be formed in the oxidative cleavage at C4 positions in the anhydroglucose units of cellulose. The lower aldehyde content in the fibres treated with the mixture of *Tr* AA9A and *Pa* AA9E (1 +1 mg/g dry fibre) compared to treatment with only *Tr* AA9A (2 mg enzyme/g dry fibre) was presumably caused by the two times lower amount of C4 oxidising activity in the mixture (1 mg *Tr* AA9A/g dry fibre) or competition for co-substrate (s) and/or reductant between the *Tr* AA9A with *Pa* AA9E. The mixture of LPMOs decreased the pulp viscosity 290 mL/g (from 690 mL/g to

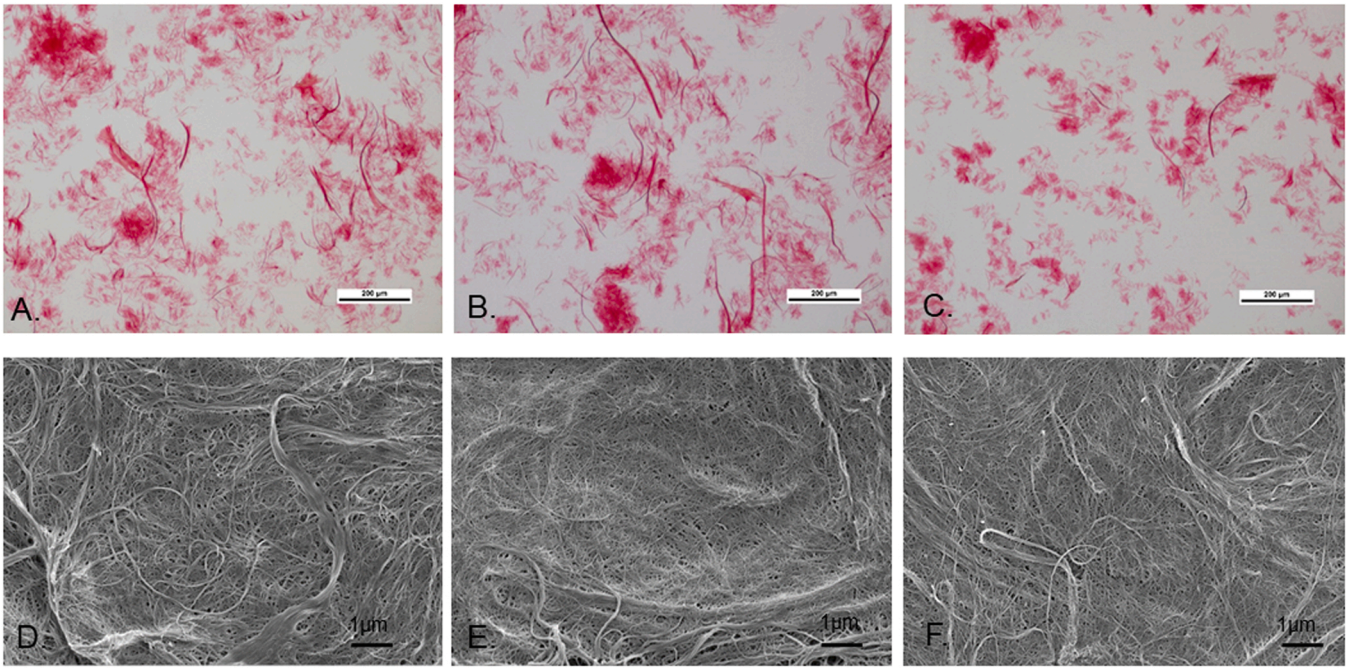

Fig. 3. Light microscopy (A.-C.) and SEM images (D.-F.) from fibrillated never-dried rSKF samples. A &D Controls where no enzyme and no GA was used in pretreatment. B&E Control where only GA was used in the pretreatment. C&F 2 mg LPMO *Tr* AA9A and 1 mM GA was used in 24 h pretreatment, at pH 7 and 45 °C.

400 mL/g), which is in the range expected from two times lower dosage of *Tr* AA9A and *Pa* AA9E. The charge of the fibres was highest when the mixture was applied (21 mmol/kg), but the difference to sole *Pa* AA9E treatment (19 mmol/kg), *Tr* AA9A treatment (18 mmol/g) and control (17 mmol/g) was very small and may arise merely from heterogeneity of the pulp.

The never dried rSKF batch 2 reference and enzyme treated samples were fibrillated in microfluidizator in the same way as batch 1 samples. Compared to the batch 1, the batch 2 reference sample and *Tr* AA9A treated sample contained clearly lower amount of residual fibres (Fig. 2B and Fig. 4A), indicating that the effects of the enzyme treatments on the fibrillation values cannot be directly compared between the batches, but relative to the reference sample in each series.

Lowest amount of residual fibres, i.e. 50% of that in the reference sample (pulp only, without GA), were measured in CNF prepared from *Pa* AA9E pretreated rSKF (Fig. 5A). The fines content was 79–87% in all the samples after six passes of fibrillation, and in this series highest fines content was found from the reference sample. The highest fines content (85–89%) in the enzyme treated samples were measured after four passes of fibrillation. This could mean that fines were further converted to smaller nano-sized fibrils in the consequent microfluidization cycles (Fig. 5C). These nano-sized fibrils could not be detected by the fibre analyser, but as a result of fibrillation the relative amount of nano-sized material increased (Fig. 5B). The variation in the fines content in this study was however quite small, and considering the optical analyses, the clearest conclusions on the enzyme effects on the fibrillation can be based on the residual micron-sized fibre content. Quantification of the amount of nanosized material with a centrifugation-based method showed that in case of *Pa* AA9E treated fibres, four fibrillation passes were sufficient to produce similar amount of nanomaterial as six passes in case of the other enzyme treatments (Fig. 5B). The ability of *Pa* AA9E to enhance fibrillation is in line with results in Moreau et al. (2019) where this enzyme was used in pretreatment of bleached birch kraft fibres. Similar trend was seen in the development of CNF gel viscosity (Fig. 5B). The apparent viscosity values of CNF can increase by increasing the degree of fibrillation, due to higher surface area and increase amount of interfibril connections (Albornoz-Palma et al., 2020). The CNF obtained from treatment with mixture of *Tr* AA9A and *Pa* AA9E was similar to CNF from *Tr* AA9A treatment, suggesting that the *Pa* AA9E dosage in the mixture was not sufficient to produce the faster fibrillation, and/or the competition between the two enzymes affected the *Pa* AA9E performance.

In earlier work by Hiltunen (2021), the purified *Tr* AA9A and *Pa* AA9E LPMOs described here were compared in capability to enhance saccharification of pretreated softwood lignocellulose by mixture of cellulases. It was seen that while addition of the *Tr* AA9A to the cellulase mixture clearly facilitated the saccharification, the *Pa* AA9E did not have such effect. This is line with results from Tokin et al. (2020) who observed that LPMOs which can hydroxylate at C4 positions in cellulose, i.e. *Ta* AA9A from *Thermoascus aurantiacus* and *Ls* AA9A from *Lentinus similis,* enhanced hydrolysis of crystalline cellulose in synergy with cellulase enzyme, while strictly C1 specific LPMO *Tt* AA9E from *Thielavia terrestris* had even impairing effect on saccharification. This suggests that regioselectivity may affect the suitability of LPMOs to different applications, and that C1 oxidising LPMOs, such as *Pa* AA9E may be better for cellulose and fibre modification than biomass saccharification in biofuel and -chemical production.

3.5. Cellulose film properties

Free-standing films were casted from fibrillated pulps produced using the LPMOs in the pretreatment, and the reference samples (prepared without enzyme and GA), in order to evaluate the material performance of the samples. The thickness of the films was ca 30 µm and sorbitol was used as plasticizing compound. Mechanical and barrier properties of the films are shown in Table 2. Measured values were in line with earlier reports on CNF films prepared from softwood fibres using similar method (Österberg et al., 2013; Vartiainen et al., 2014, 2015).

No significant difference was seen in the Young's modulus of the samples. The strength (MPa) of the CNF films prepared from pulps pretreated with *Pa* AA9E or *Tr* AA9A+*Pa* AA9E were slightly lower (110 and 101 MPa, respectively) than the in the reference films or when only *Tr* AA9A was used in the pretreatment (ca 125 MPa). The strain (%) was also somewhat lower in CNFs prepared from LPMO pretreated pulps, and again the reduction of strain was largest when *Pa* AA9E was

Table 1
Gluco- and xylo-oligosaccharides formed in the enzymatic treatments (DP2-DP4, mg/L).

Sample	Glc2	Glc2-AldA	Glc2-diolC4	Glc2-KetoneC4	Glc2-DoubleOx	Glc3	Glc3-AldA	Glc3-diolC4	Glc3-KetoneC4	Glc3-DoubleOx	Glc4	Glc4-AldA	Glc4-diolC4	Glc4-KetoneC4	Glc4-DoubleOx
No enzyme and GA															
Tr AA9A	6.6	3.3	25.1	5.1		25.1	2.2	12.6	6.6		35.5	2.9	12.6	9.6	1.4
Pa AA9E	0.3	21.0			3.7	0.5	24.1			5.2	4.0	39.4			7.8
Tr AA9A+ *Pa* AA9E	1.7	15.1	4.4	1.5		17.5	17.8	4.3	0.9		45.2	29.0		1.6	7.1
Sample	**X2**	**X2-AldA**	**X2-diolC4**	**X2-KetoneC4**	**X2-DoubleOx**	**X3**	**X3 -AldA**	**X3-diolC4-**	**X3-KetoneC4**	**X3-DoubleOx**	**X4**	**X4 -AldA-**	**X4-diolC4-**	**X4-KetoneC4**	**X4-DoubleOx**
No enzyme and GA	0.50					0.20									
Tr AA9A	0.50	0.30	0.50	0.30	17.50	0.80		0.20			1.50		0.30		
Pa AA9E	1.50	0.30	0.20			10.20	0.90	2.50		0.20	12.50	2.10	3.40	0.20	0.60
Tr AA9A+ *Pa* AA9E	0.90	0.30	0.30	0.30	2.00	4.50	0.20	1.20			5.80	0.60	1.80		

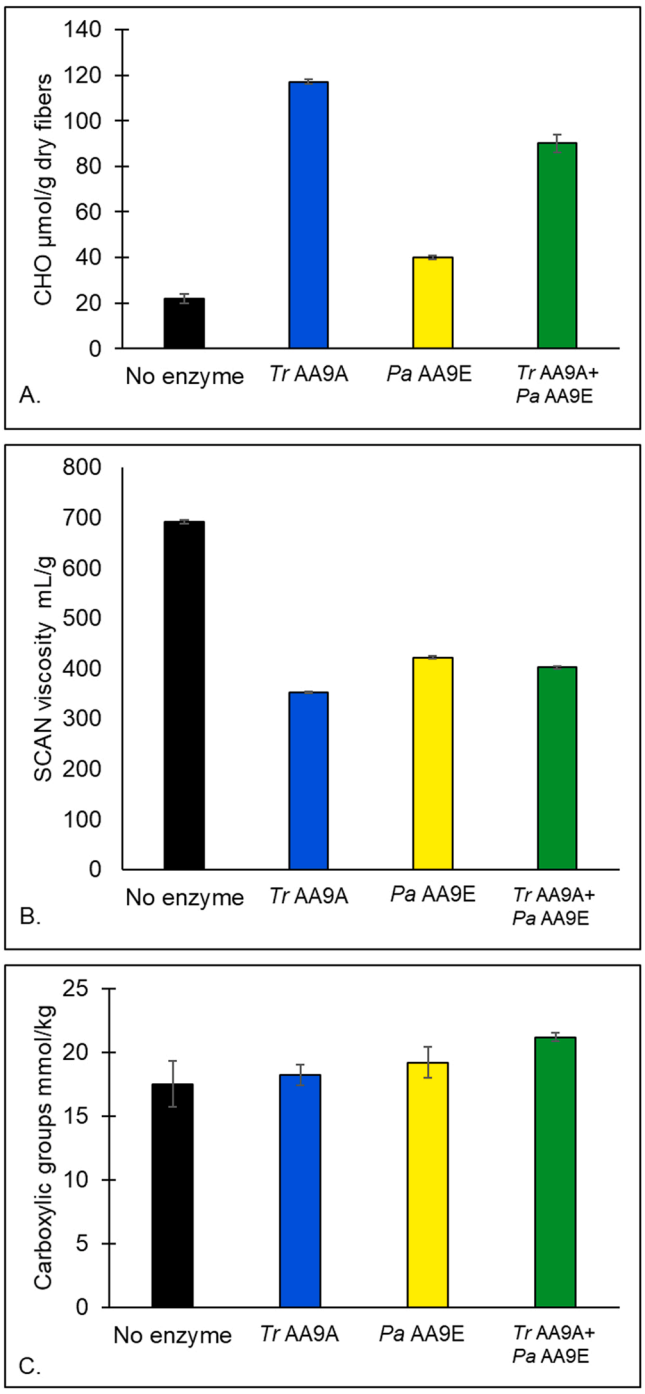

Fig. 4. Comparison *Tr* AA9A and *Pa* AA9E in oxidation of pre-refined never-dried rSKF (batch 2). The amount of aldehydes in pulp (A),the intrinsic (SCAN) viscosity of pulp samples (B), and charge of the pulp samples analysed with conductometric titration (C). The enzyme treatment was carried out using 2 mg enzyme/g dry fibre, at 1.5% solids loading, pH 7 and 45 °C for 24 h.

included in the pretreatment. In Koskela et al. (2019), clearly higher tensile strength (ca 260 MPa) was observed in nanopapers prepared from LPMO (C1 oxidizing) treated and mechanically fibrillated softwood holocellulose, compared to nanopaper prepared without enzymatic pretreatment (ca 150 MPa). The improved strength was proposed to be caused by better the fibrillation of LPMO treated samples: without the LPMO treatment the holocelluloses remained intact in the mild Ultra-Turrax treatment used in the fibrillation (Koskela et al., 2019). The minor effect of LPMO treatment in the strength of CNF films prepared

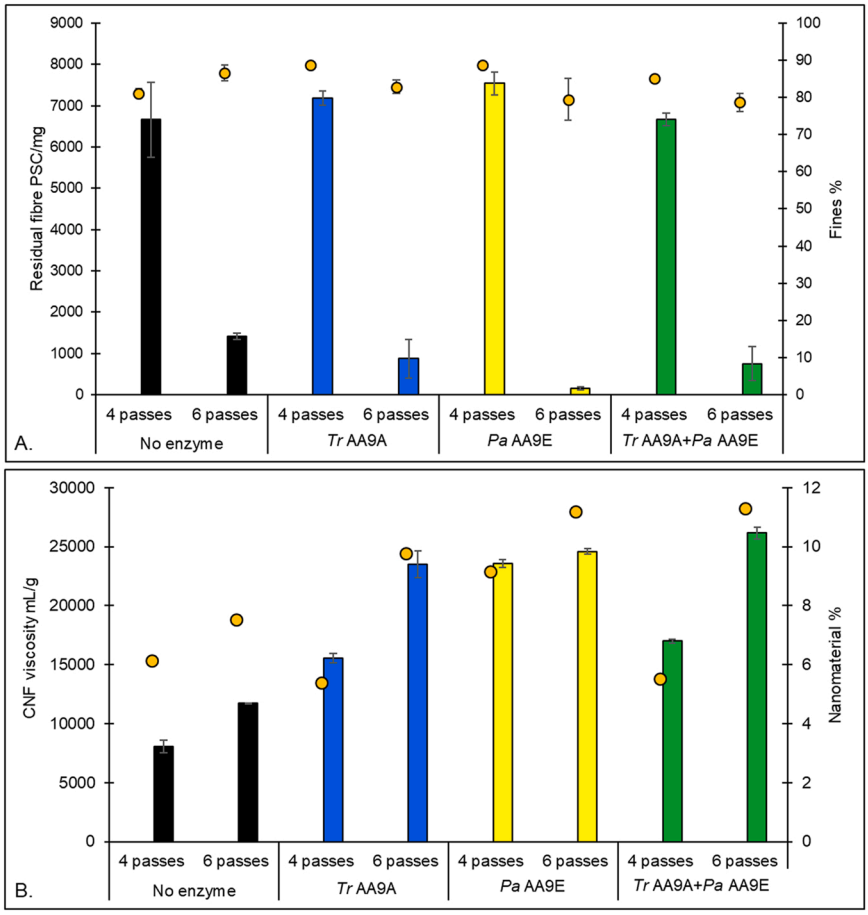

Fig. 5. Effect of LPMO *Tr* AA9A and *Pa* AA9E pretreatment on nanofibrillation of never-dried rSKF (batch 2). The fibrillation was carried out by microfluidization (total 4 or 6 passes of fibrillation). A. The fibrillation was followed by quantifying residual fibres (PSC/mg, columns) and fines (%, dots) in CNF. B. The nanosized material in the fibrillated CNF samples (%, dots) was quantified with a centrifugation base-method and gel viscosity (mPa*s, columns) was analysed with Brookfield rheometer.

Table 2
Properties of the self-standing films prepared from the fibrillated LPMO pretreated softwood kraft fibres.

Sample	Thickness	Y-Modulus	Strength	Strain	OTR	WVTR
	µm	MPa	MPa	%	cc/(m^2 *day)	g/(m^2 *day)
No enzyme	29 ± 1.0	3874 ± 171	125 ± 8	13.3 ± 0.9	0.9 ± 0	11.7 ± 1.4
Tr AA9A	30 ± 0.8	4020 ± 159	127.4 ± 6	11.9 ± 0.6	1.1 ± 0	20.4 ± 3.1
Pa AA9E	29 ± 1.2	3954 ± 274	110.6 ± 1.2	10.9 ± 1.2	1.2 ± 0	22.6 ± 6.0
Tr AA9A + *Pa* AA9E	29 ± 1.6	4066 ± 225	101.8 ± 12	9 ± 2.3	1.0 ± 0.1	20.5 ± 0.1

from softwood pulp in our study may have caused by the employed pulp and enzyme combination, different degree of fibrillation as well as different fibrillation method utilised, as well as by usage of sorbitol in the film preparation, which is known to affect the mechanical and barrier properties of the CNF films (Aulin et al., 2022).

The oxygen transmission rate (OTR) of all the films were very close to each other, ca 1 cc/(m^2 *day), which is in line with published value of CNF films plasticized with sorbitol (Aulin et al., 2022). The water vapour transmission rate (WVTR) of the films prepared from LPMO treated pulps were instead two times higher than in the reference. The WVTR of CNF films can be affected by crystallinity, hemicellulose content and porosity of the CNF films (Wang et al., 2018). Considering the similar oxygen barrier properties, higher porosity may not be likely explanation for the change in the WVTR, and degradation of hemicellulose would be expected to translate into lower WVTR. Crystallinity values were not determined in the current work, but based on current understanding on the mode of action of the AA9 family LPMOs, oxidative degradation of crystalline areas in fibres seems plausible. Furthermore, Kim et al. (2021) have recently compared water vapour permeation of CNF films prepared from bleached hardwood after enzymatic hydrolysis, TEMPO-oxidation or carboxymethylation. They observed that the CNF films prepared from endoglucanase pretreated fibres exhibited lowest water vapour permeation, which was assumed to be due to higher crystallinity of the films after endoglucanase catalysed hydrolysis of disordered areas in the fibres.

4. Conclusions

Enzymatic oxidation, catalysed by two different types of fungal AA9 family LPMO enzymes alone and in combination, was studied as a pretreatment method in CNF production from bleached softwood fibres with industrially relevant mechanical disintegrators. The LPMO enzymes had clear effect on lowering the viscosity of the pre-refined fibres, presumably due to better accessibility compared to non-refined fibres. The treatment with C4 hydroxylating LPMO *Tr* AA9A resulted in higher aldehyde content in the pulp, while surprisingly no increase in charge was produced with the C1 oxidising LPMO *Pa* AA9E. Both LPMOs facilitated the fibrillation in microfluidization, and the *Pa* AA9E treatment resulted in faster fibrillation than the *Tr* AA9A treatment. Combined treatment with *Tr* AA9A and *Pa* AA9E did not give any additional benefit in fibrillation. The free standing cellulose films casted from LPMO pretreated and fibrillated pulps exhibited similar mechanical strength and oxygen barrier properties as the reference films. These

results are promising. In order to further optimise this methodology for larger scale applications, enzyme selection (e.g. using C1-oxidising LPMO enzyme without a CBM) and/or optimized provision of the hydrogen peroxide as oxygen donor (instead of molecular oxygen) should be considered. The effect of the LPMO pretreatment on water vapour permeation of the films would also need some further studies in order to allow proper control of the barrier properties.

CRediT authorship contribution statement

Kaisa Marjamaa: Supervision of enzyme purification and analyses, design of the fibre treatments and analyses, interpretation of the results and writing of the manuscript. Panu Lahtinen: contribution to design of the fibre treatment and analyses; designed and supervised the CNF production and their analyses and CNF films and their analyses; contributed interpretation of the results and writing of the manuscript. Suvi Arola: contributed to the design of the fibre treatment and analyses, CNF production and CNF films analyses; contributed interpretation of the results. Natalia Maiorova and Heli Nygren: analysis of the soluble oxidation products. Nina Aro: Supervision of *Trichoderma* strain construction and enzyme production. Anu Koivula: Contributed to the planning of the work from enzyme production to fibrillation trials, interpretation of the results and writing of the manuscript.

Declaration of Competing Interest

The authors declare that they have no known competing financial interests or personal relationships that could have appeared to influence the work reported in this paper.

Data Availability

Data will be made available on request.

Acknowledgement

We thank Riitta Isoniemi, Mariitta Svanberg, Nina Vihersola, Mari Leino, Ulla Salonen, Katja Pettersson, Susanne Barcker and Kirsi Kiiveri (VTT) for technical assistance. The work was funded the Academy of Finland's Flagship Programme under Projects No. 318890 and 318891 (Competence Center for Materials Bioeconomy, FinnCERES), Business Finland BioAd-FiDiPro project (Dnro 1918/31/2015) and project FunEnzFibres, which is funded under the umbrella of ERA-NET Cofund ForestValue by Academy of Finland (grant number 326359). ForestValue has received funding from the European Union's Horizon 2020 research and innovation programme under grant agreement N° 773324. Suci Arola was funded by the Academy of Finland postdoc funding (grant number 326262).

References

Ahola, S., Salmi, J., Johansson, L.S., Laine, J., Osterberg, M., 2008. Model films from native cellulose nanofibrils. Prep., swelling, Surf. Interact. Biomacromol. 9, 1273–1282. https://doi.org/10.1021/bm701317k.

Albornoz-Palma, G., Betancourt, F., Teixeira Mendonça, R., Chinga-Carrasco, G., Pereira, M., 2020. Relationship between rheological and morphological characteristics of cellulose nanofibrils in dilute dispersions. Carbohydr. Polym. 230, 115588 https://doi.org/10.1016/j.carbpol.2019.115588.

de Amorim, J.D.P., de Souza, K.C., Duarte, C.R., da Silva Duarte, I., de Assis Sales Ribeiro, F., Silva, G.S., de Farias, P.M.A., Stingl, A., Costa, A.F.S., Vinhas, G.M., Sarubbo, L.A., 2020. Plant and bacterial nanocellulose: production, properties and applications in medicine, food, cosmetics, electronics and engineering. A review. Environ. Chem. Lett. 18, 851–869. https://doi.org/10.1007/s10311-020-00989-9.

Aulin, C., Ahok, S., Josefsson, P., Nishino, T., Hirose, Y., Österberg, M., Wågberg, L., 2009. Nanoscale cellulose films with different crystallinities and mesostructures - Their surface properties and interaction with water. Langmuir 25, 7675–7685. https://doi.org/10.1021/la900323n.

Aulin, C., Johansson, E., Wågberg, L., Lindström, T., 2010. Self-organized films from cellulose i nanofibrils using the layer-by-layer technique. Biomacromolecules 11, 872–882. https://doi.org/10.1021/bm100075e.

Aulin, C., Flodberg, G., Ström, G., Lindström, T., 2022. Enhanced mechanical and gas barrier performance of plasticized cellulose nanofibril films. Nord Pulp Pap. Res J. 37, 138–148. https://doi.org/10.1515/npprj-2021-0061.

Bennati-Granier, C., Garajova, S., Champion, C., Grisel, S., Haon, M., Zhou, S., Fanuel, M., Ropartz, D., Rogniaux, H., Gimbert, I., Record, E., Berrin, J.-G., 2015. Substrate specificity and regioselectivity of fungal AA9 lytic polysaccharide monooxygenases secreted by Podospora anserina. Biotechnol. Biofuels 8, 90. https://doi.org/10.1186/s13068-015-0274-3.

Bissaro, B., Røhr, Å.K., Müller, G., Chylenski, P., Skaugen, M., Forsberg, Z., Horn, S.J., Vaaje-Kolstad, G., Eijsink, V.G.H., 2017. Oxidative cleavage of polysaccharides by monocopper enzymes depends on H_2O_2. Nat. Chem. Biol. 13, 1123–1128. https://doi.org/10.1038/nchembio.2470.

Cannella, D., Möllers, K.B., Frigaard, N.U., Jensen, P.E., Bjerrum, M.J., Johansen, K.S., Felby, C., 2016. Light-driven oxidation of polysaccharides by photosynthetic pigments and a metalloenzyme. Nat. Commun. 7, 1–8. https://doi.org/10.1038/ncomms11134.

Ceccherini, S., Rahikainen, J., Marjamaa, K., Sawada, D., Grönqvist, S., Maloney, T., 2021. Activation of softwood Kraft pulp at high solids content by endoglucanase and lytic polysaccharide monooxygenase. Ind. Crops Prod. 166, 113463 https://doi.org/10.1016/j.indcrop.2021.113463.

Chalak, A., Villares, A., Moreau, C., Haon, M., Grisel, S., D'Orlando, A., Herpoël-Gimbert, I., Labourel, A., Cathala, B., Berrin, J.G., 2019. Influence of the carbohydrate-binding module on the activity of a fungal AA9 lytic polysaccharide monooxygenase on cellulosic substrates. Biotechnol. Biofuels 12, 1–10. https://doi.org/10.1186/s13068-019-1548-y.

Colot, H.V., Park, G., Turner, G.E., Ringelberg, C., Crew, C.M., Litvinkova, L., Weiss, R.L., Borkovich, K.A., Dunlap, J.C., 2006. A high-throughput gene knockout procedure for Neurospora reveals functions for multiple transcription factors. Proc. Natl. Acad. Sci. U. S. A 103, 10352–10357. https://doi.org/10.1073/pnas.0601456103.

Duan, C., Long, Y., Li, J., Ma, X., Ni, Y., 2015. Changes of cellulose accessibility to cellulase due to fiber hornification and its impact on enzymatic viscosity control of dissolving pulp. Cellulose 22, 2729–2736. https://doi.org/10.1007/s10570-015-0636-9.

Fang, W., Paananen, A., Vitikainen, M., Koskela, S., Westerholm-Parvinen, A., Joensuu, J.J., Landowski, C.P., Penttilä, M., Linder, M.B., Laaksonen, P., 2017. Elastic and pH-responsive hybrid interfaces created with engineered resilin and nanocellulose. Biomacromolecules 18, 1866–1873. https://doi.org/10.1021/acs.biomac.7b00294.

Frandsen, K.E.H., Simmons, T.J., Dupree, P., Poulsen, J.N., Hemsworth, G.R., Ciano, L., Johnston, E.M., Tovborg, M., Johansen, K.S., von Freiesleben, P., Marmuse, L., Fort, S., Cottaz, S., Driguez, H., Henrissat, B., Lenfant, N., Tuna, F., Baldansuren, A., Davies, G.J., Lo Leggio, L., Walton, P.H., 2016. The molecular basis of polysaccharide cleavage by lytic polysaccharide monooxygenases. Nat. Chem. Biol. 12, 298–303. https://doi.org/10.1038/nchembio.2029.

Grönqvist, S., Hakala, T.K., Kamppuri, T., Liitia, T., Vehviläinen, M., Maloney, T., Suurnäkki, A., 2014. Fibre porosity development of dissolving pulp during mechanical and enzymatic processing. Cellulose 21, 3667–3676. https://doi.org/10.1007/s10570-014-0352-x.

Hansson, H., Karkehabadi, S., Mikkelsen, N., Douglas, N.R., Kim, S., Lam, A., Kaper, T., Kelemen, B., Meier, K.K., Jones, S.M., Solomon, E.I., Sandgren, M., 2017. High-resolution structure of a lytic polysaccharide monooxygenase from Hypocrea jecorina reveals a predicted linker as an integral part of the catalytic domain. J. Biol. Chem. 292, 19099–19109. https://doi.org/10.1074/jbc.M117.799767.

Harris, P.V., Welner, D., Mcfarland, K.C., Re, E., Poulsen, J.N., Brown, K., Salbo, R., Ding, H., Vlasenko, E., Merino, S., Xu, F., Cherry, J., Larsen, S., Leggio, L.Lo, 2010. Stimul. Lignocellul. Biomass-.-. Hydrolys. Proteins Glycoside Hydrolase Fam. 61: Struct. Funct. a Large, Enigmatic Fam. † 3305–3316. https://doi.org/10.1021/bi100009p.

Hemsworth, G.R., Johnston, E.M., Davies, G.J., Walton, P.H., 2015. Lytic Polysaccharide Monooxygenases in Biomass Conversion. Trends Biotechnol. 33, 747–761. https://doi.org/10.1016/j.tibtech.2015.09.006.

Henriksson, M., Henriksson, G., Berglund, L.A., Lindström, T., 2007. An environmentally friendly method for enzyme-assisted preparation of microfibrillated cellulose (MFC) nanofibers. Eur. Polym. J. 43, 3434–3441. https://doi.org/10.1016/j.eurpolymj.2007.05.038.

Hiltunen, M., 2021. Characterization of the auxiliary activity enzymes Trichoderma reesei Tr AA3_2, Tr AA9A and Podospora anserina Pa AA9E, with potential roles in cellulose modification. Master's thesis. University of Jyväskylä, Finland.

Hu, J., Tian, D., Renneckar, S., Saddler, J.N., 2018. Enzyme mediated nanofibrillation of cellulose by the synergistic actions of an endoglucanase, lytic polysaccharide monooxygenase (LPMO) and xylanase. Sci. Rep. 8, 4–11. https://doi.org/10.1038/s41598-018-21016-6.

Hubbe, M.A., Tayeb, P., Joyce, M., Tyagi, P., Kehoe, M., Dimic-Misic, K., Pal, L., 2017. Rheology of nanocellulose-rich aqueous suspensions: a review. BioRes 12, 9556–9661.

Hüttner, S., Várnai, A., Petrović, D.M., Bach, C.X., Kim Anh, D.T., Thanh, V.N., Eijsink, V. G.H., Larsbrink, J., Olsson, L., 2019. Specific xylan activity revealed for AA9 lytic polysaccharide monooxygenases of the thermophilic fungus malbranchea cinnamomea by functional characterization. Appl. Environ. Microbiol. 85, e01408–e01419. https://doi.org/10.1128/AEM.01408-19.

Imai, M., Furujo, A., Sugiyama, J., 2019. Direct observation of cellulase penetration in oven-dried pulp by confocal laser scanning microscopy. Cellulose 26, 7653–7662. https://doi.org/10.1007/s10570-019-02676-7.

Isogai, A., 2018. Review Development of completely dispersed cellulose nano fi bers. Proc. Jpn. Acad., Ser. B 94 (94), 161–179.

Isogai, A., Saito, T., Fukuzumi, H., 2011. TEMPO-oxidized cellulose nanofibers. Nanoscale 3, 71–85. https://doi.org/10.1039/c0nr00583e.

Kangas, Felissia, Filgueira, Ehman, Vallejos, Imlauer, Lahtinen, Area, Chinga-Carrasco, 2019. 3D printing high-consistency enzymatic nanocellulose obtained from a Soda-Ethanol-O2 pine sawdust pulp. Bioengineering 6, 60. https://doi.org/10.3390/bioengineering6030060.

Karlsson, J., Saloheimo, M., Siika-aho, M., Tenkanen, M., Penttila, M., 2001. Homologous expression and characterization of Cel61A (EG IV) of Trichoderma reesei. Eur. J. Biochem. 6507, 6498–6507.

Kim, H.J., Roy, S., Rhim, J.W., 2021. Effects of various types of cellulose nanofibers on the physical properties of the CNF-based films. J. Environ. Chem. Eng. 9, 106043 https://doi.org/10.1016/j.jece.2021.106043.

Kont, R., Pihlajaniemi, V., Borisova, A.S., Aro, N., Marjamaa, K., Loogen, J., Büchs, J., Eijsink, V.G.H., Kruus, K., Väljamaë, P., 2019. The liquid fraction from hydrothermal pretreatment of wheat straw provides lytic polysaccharide monooxygenases with both electrons and H_2O_2 co-substrate. Biotechnol. Biofuels 12. https://doi.org/10.1186/s13068-019-1578-5.

Kont, R., Bissaro, B., Eijsink, V.G.H., Väljamäe, P., 2020. Kinetic insights into the peroxygenase activity of cellulose-active lytic polysaccharide monooxygenases (LPMOs). Nat. Commun. 11. https://doi.org/10.1038/s41467-020-19561-8.

Koskela, S., Wang, S., Xu, D., Yang, X., Li, K., Berglund, L.A., McKee, L.S., Bulone, V., Zhou, Q., 2019. Lytic polysaccharide monooxygenase (LPMO) mediated production of ultra-fine cellulose nanofibres from delignified softwood fibres. Green. Chem. 21, 5924–5933. https://doi.org/10.1039/c9gc02808k.

Lahtinen, P., Liukkonen, S., Pere, J., Sneck, A., Kangas, H., 2014. A Comparative study of fibrillated fibers from different mechanical and chemical pulps. BioResources 9, 2115–2127. https://doi.org/10.15376/biores.9.2.2115-2127.

Landowski, C.P., Huuskonen, A., Wahl, R., Westerholm-Parvinen, A., Kanerva, A., Hänninen, A.L., Salovuori, N., Penttilä, M., Natunen, J., Ostermeier, C., Helk, B., Saarinen, J., Saloheimo, M., 2015. Enabling low cost biopharmaceuticals: a systematic approach to delete proteases from a well-known protein production host trichoderma reesei. PLoS One 10, 1–28. https://doi.org/10.1371/journal.pone.0134723.

Langston, J.A., Shaghasi, T., Abbate, E., Xu, F., Vlasenko, E., Sweeney, M.D., 2011. Oxidoreductive cellulose depolymerization by the enzymes cellobiose dehydrogenase and glycoside hydrolase 61. Appl. Environ. Microbiol. 77, 7007–7015. https://doi.org/10.1128/AEM.05815-11.

Liimatainen, H., Visanko, M., Sirviö, J.A., Hormi, O.E.O., Niinimaki, J., 2012. Enhancement of the nanofibrillation of wood cellulose through sequential periodate-chlorite oxidation. Biomacromolecules 13, 1592–1597. https://doi.org/10.1021/bm300319m.

Liimatainen, H., Visanko, M., Sirviö, J., Hormi, O., Niinimäki, J., 2013. Sulfonated cellulose nanofibrils obtained from wood pulp through regioselective oxidative bisulfite pre-treatment. Cellulose 20, 741–749. https://doi.org/10.1007/s10570-013-9865-y.

Lo Leggio, L., Simmons, T.J., Poulsen, J.C.N., Frandsen, K.E.H., Hemsworth, G.R., Stringer, M.A., Von Freiesleben, P., Tovborg, M., Johansen, K.S., De Maria, L., Harris, P.V., Soong, C.L., Dupree, P., Tryfona, T., Lenfant, N., Henrissat, B., Davies, G.J., Walton, P.H., 2015. Structure and boosting activity of a starch-degrading lytic polysaccharide monooxygenase. Nat. Commun. 6. https://doi.org/10.1038/ncomms6961.

Marjamaa, K., Kruus, K., 2018. Enzyme biotechnology in degradation and modification of plant cell wall polymers. Physiol. Plant. 164, 106–118. https://doi.org/10.1111/ppl.12800.

Marjamaa, K., Rahikainen, J., Karjalainen, M., Maiorova, N., Holopainen-Mantila, U., Molinier, M., Aro, N., Nygren, H., Mikkelson, A., Koivula, A., Kruus, K., 2022. Oxidative modification of cellulosic fibres by lytic polysaccharide monooxygenase AA9A from *Trichoderma reesei*. Cellulose 29, 6021–6038. https://doi.org/10.1007/s10570-022-04648-w.

Meier, K.K., Jones, S.M., Kaper, T., Hansson, H., Koetsier, M.J., Karkehabadi, S., Solomon, E.I., Sandgren, M., Kelemen, B., 2018. Oxygen activation by Cu LPMOs in recalcitrant carbohydrate polysaccharide conversion to monomer sugars. Chem. Rev. 118, 2593–2635. https://doi.org/10.1021/acs.chemrev.7b00421.

Moreau, C., Tapin-Lingua, S., Grisel, S., Gimbert, I., Le Gall, S., Meyer, V., Petit-Conil, M., Berrin, J.G., Cathala, B., Villares, A., 2019. Lytic polysaccharide monooxygenases (LPMOs) facilitate cellulose nanofibrils production. Biotechnol. Biofuels 12, 13–17. https://doi.org/10.1186/s13068-019-1501-0.

Müller, G., Várnai, A., Johansen, K.S., Eijsink, V.G.H., Horn, S.J., 2015. Harnessing the potential of LPMO-containing cellulase cocktails poses new demands on processing conditions. Biotechnol. Biofuels 8, 187. https://doi.org/10.1186/s13068-015-0376-y.

Nazhad, M.M., Ramos, L.P., Paszner, L., Saddler, J.N., 1995. Structural constraints affecting the initial enzymatic hydrolysis of recycled paper. Enzym. Microb. Technol. 17, 68–74. https://doi.org/10.1016/0141-0229(94)00057-X.

Nechyporchuk, O., Belgacem, M.N., Bras, J., 2016. Production of cellulose nanofibrils: a review of recent advances. Ind. Crops Prod. 93, 2–25. https://doi.org/10.1016/j.indcrop.2016.02.016.

Nie, S., Zhang, K., Lin, X., Zhang, C., Yan, D., Liang, H., Wang, S., 2018a. Enzymatic pretreatment for the improvement of dispersion and film properties of cellulose nanofibrils. Carbohydr. Polym. 181, 1136–1142. https://doi.org/10.1016/j.carbpol.2017.11.020.

Nie, S., Zhang, C., Zhang, Q., Zhang, K., Zhang, Y., Tao, P., Wang, S., 2018b. Enzymatic and cold alkaline pretreatments of sugarcane bagasse pulp to produce cellulose nanofibrils using a mechanical method. Ind. Crops Prod. 124, 435–441. https://doi.org/10.1016/j.indcrop.2018.08.033.

Obolenskaya, A.V., Elnitskaya, Z.P., Leonovitch, A.A., 1991. Determination of aldehyde groups in oxidized pulps. Laboratory Manipulations in Wood and Cellulose Chemistry. Ecologia, Moscow, pp. 211–212.

Østby, H., Hansen, L.D., Horn, S.J., Eijsink, V.G.H., Várnai, A., 2020. Enzymatic processing of lignocellulosic biomass: principles, recent advances and perspectives. Journal of Industrial Microbiology and Biotechnology. Springer International Publishing. https://doi.org/10.1007/s10295-020-02301-8.

Österberg, M., Vartiainen, J., Lucenius, J., Hippi, U., Seppälä, J., Serimaa, R., Laine, J., 2013. A fast method to produce strong NFC films as a platform for barrier and functional materials. ACS Appl. Mater. Interfaces 5, 4640–4647. https://doi.org/10.1021/am401046x.

Pääkko, M., Ankerfors, M., Kosonen, H., Nykänen, A., Ahola, S., Österberg, M., Ruokolainen, J., Laine, J., Larsson, P.T., Ikkala, O., Lindström, T., 2007. Enzymatic hydrolysis combined with mechanical shearing and high-pressure homogenization for nanoscale cellulose fibrils and strong gels. Biomacromolecules 8, 1934–1941. https://doi.org/10.1021/bm061215p.

Penttilä, M., Nevalainen, H., Rättö, M., Salminen, E., Knowles, J., 1987. A versatile transformation system for the cellulolytic filamentous fungus *Trichoderma reesei*. Gene 61, 155–164. https://doi.org/10.1016/0378-1119(87)90110-7.

Pierce, B.C., Wittrup, J., Wichmann, J., Meyer, A.S., 2017. Oxidative cleavage and hydrolytic boosting of cellulose in soybean spent flakes by Trichoderma reesei Cel61A lytic polysaccharide monooxygenase. Enzym. Microb. Technol. 98, 58–66. https://doi.org/10.1016/j.enzmictec.2016.12.007.

Pirich, C.L., Picheth, G.F., Fontes, A.M., Delgado-Aguilar, M., Ramos, L.P., 2020. Disruptive enzyme-based strategies to isolate nanocelluloses: a review. Cellulose 27, 5457–5475. https://doi.org/10.1007/s10570-020-03185-8.

Quinlan, R.J., Sweeney, M.D., Lo, L., Otten, H., Poulsen, J.N., Tryfona, T., Walter, C.P., Dupree, P., Xu, F., Davies, G.J., Walton, P.H., 2011. Insights into the oxidative degradation of cellulose by a copper metalloenzyme that exploits biomass components. https://doi.org/10.1073/pnas.1105776108.

Rahikainen, J., Ceccherini, S., Molinier, M., Holopainen-Mantila, U., Reza, M., Väisänen, S., Puranen, T., Kruus, K., Vuorinen, T., Maloney, T., Suurnäkki, A., Grönqvist, S., 2019. Effect of cellulase family and structure on modification of wood fibres at high consistency. Cellulose 26, 5085–5103. https://doi.org/10.1007/s10570-019-02424-x.

Saito, T., Nishiyama, Y., Putaux, J.L., Vignon, M., Isogai, A., 2006. Homogeneous suspensions of individualized microfibrils from TEMPO-catalyzed oxidation of native cellulose. Biomacromolecules 7, 1687–1691. https://doi.org/10.1021/bm060154s.

Saloheimo, M., Nakari-Setala, T., Tenkanen, M., Penttila, M., 1997. cDNA cloning of a *Trichoderma reesei* cellulase and demonstration of endoglucanase activity by expression in yeast. Eur. J. Biochem 249, 584–591.

Song, B., Li, B., Wang, X., Shen, W., Park, S., Collings, C., Feng, A., Smith, S.J., Walton, J. D., Ding, S.Y., 2018. Real-time imaging reveals that lytic polysaccharide monooxygenase promotes cellulase activity by increasing cellulose accessibility. Biotechnol. Biofuels 11, 1–11. https://doi.org/10.1186/s13068-018-1023-1.

Swerin, A., Odberg, L., Lindström, T., 1990. Deswelling of hardwood kraft pulp fibers by cationic polymers: the effect on wet pressing and sheet properties. Nord. Pulp Pap. Res. J. 5, 188–196. https://doi.org/10.3183/npprj-1990-05-04-p188-196.

Tammelin, T., Salminen, A. and Hippi, U. 2011. Method for the preparation of NFC films on supports, Patent FI20116048.

Tanghe, M., Danneels, B., Camattari, A., Glieder, A., Vandenberghe, I., Devreese, B., Stals, I., Desmet, T., 2015. Recombinant expression of trichoderma reesei Cel61A in Pichia pastoris: optimizing yield and N-terminal processing. Mol. Biotechnol. 57, 1010–1017. https://doi.org/10.1007/s12033-015-9887-9.

Tokin, R., Ipsen, J.Ø., Westh, P., Johansen, K.S., 2020. The synergy between LPMOs and cellulases in enzymatic saccharification of cellulose is both enzyme- and substrate-dependent. Biotechnol. Lett. 42, 1975–1984. https://doi.org/10.1007/s10529-020-02922-0.

Vaaje-Kolstad, G., Westereng, B., Horn, S.J., Liu, Z., Zhai, H., Sørlie, M., Eijsink, V.G.H., 2010. An oxidative enzyme boosting the enzymatic conversion of recalcitrant polysaccharides. Science 330, 219–222. https://doi.org/10.1126/science.1192231.

Vartiainen, J., Vähä-Nissi, M., Harlin, A., 2014. Biopolymer films and coatings in packaging applications - a review of recent de-velopments. Mater. Sci. Appl. 5, 708–718. https://doi.org/10.4236/msa.2014.510072.

Vartiainen, J., Lahtinen, P., Kaljunen, T., Kunnari, V., Peresin, M.S., Tammelin, T., 2015. Comparison of properties between cel-lulose nanofibrils made from banana, sugar beet, hemp, softwood and harwood pulps. O Pap. 76, 57–60. http://www.revistaopapel.org.br/noticia-anexos/1426614602_5a503d2f8ab484a0ed1af63e04f99184_295901872.pdf.

Vartiainen, J., Pelto, J., Kaljunen, T., Kenttä, E., 2016. Hydrophobization of cellophane and cellulose nanofibrils films by supercritical state carbon dioxide impregnation with walnut oil. Nord. Pulp Pap. Res. J. 31, 541–547. https://doi.org/10.3183/npprj-2016-31-04-p541-547.

Villares, A., Moreau, C., Bennati-Granier, C., Garajova, S., Foucat, L., Falourd, X., Saake, B., Berrin, J.-G., Cathala, B., 2017. Lytic polysaccharide monooxygenases disrupt the cellulose fibers structure. Sci. Rep. 7, 40262. https://doi.org/10.1038/srep40262.

Wang, J., Gardner, D.J., Stark, N.M., Bousfield, D.W., Tajvidi, M., Cai, Z., 2018. Moisture and oxygen barrier properties of cellulose nanomaterial-based films. ACS Sustain. Chem. Eng. 6, 49–70. https://doi.org/10.1021/acssuschemeng.7b03523.

Wang, W., Mozuch, M.D., Sabo, R.C., Kersten, P., Zhu, J.Y., Jin, Y., 2015. Production of cellulose nanofibrils from bleached eucalyptus fibers by hyperthermostable endoglucanase treatment and subsequent microfluidization (https://doi.org). Cellulose 22, 351–361. https://doi.org/10.1007/s10570-014-0465-2.